Cellular Microbiology (2014) **16**(5), 687–700
doi:10.1111/cmi.12212
First published online 30 September 2013

# Sequestration and histopathology in *Plasmodium chabaudi* malaria are influenced by the immune response in an organ-specific manner

**Thibaut Brugat,[1] Deirdre Cunningham,[1] Jan Sodenkamp,[1] Stephanie Coomes,[2] Mark Wilson,[2] Philip J. Spence,[1] William Jarra,[1] Joanne Thompson,[3] Cheryl Scudamore[4] and Jean Langhorne[1]***

[1]*Division of Parasitology, MRC National Institute for Medical Research, London NW7 1AA, UK.*
[2]*Division of Molecular Immunology, MRC National Institute for Medical Research, London NW7 1AA, UK.*
[3]*Institute of Immunology and Infection Research, Centre for Immunity, Infection and Evolution, School of Biological Sciences, University of Edinburgh, Edinburgh EH9 3JT, UK.*
[4]*Mary Lyons Centre, MRC Harwell, Oxfordshire OX11 0RD, UK.*

## Summary

**Infection with the malaria parasite, *Plasmodium*, is associated with a strong inflammatory response and parasite cytoadhesion (sequestration) in several organs. Here, we have carried out a systematic study of sequestration and histopathology during infection of C57Bl/6 mice with *Plasmodium chabaudi* AS and determined the influence of the immune response. This parasite sequesters predominantly in liver and lung, but not in the brain, kidney or gut. Histopathological changes occur in multiple organs during the acute infection, but are not restricted to the organs where sequestration takes place. Adaptive immunity, and signalling through the IFNγ receptor increased sequestration and histopathology in the liver, but not in the lung, suggesting that there are differences in the adhesion molecules and/or parasite ligands utilized and mechanisms of pathogenesis in these two organs. Exacerbation of pro-inflammatory responses during infection by deletion of the *il10* gene results in the aggravation of damage to lung and kidney irrespective of the degree of sequestration. The immune response therefore affected both sequestration and histopathology in an organ-specific manner. *P. chabaudi* AS provides a good model to investigate the influence of the host response on the sequestration and specific organ pathology, which is applicable to human malaria.**

Received 20 May, 2013; revised 26 July, 2013; accepted 26 August, 2013. *For correspondence. E-mail jlangho@nimr.mrc.ac.uk; Tel. (+44) 208 816 2558; Fax (+44) 208 816 2638.
Statement of equal author contribution: T.B and D.C. contributed equally to this study.


## Introduction

Infected red blood cells (iRBC) of many species of the malaria parasite *Plasmodium* adhere to endothelial cells (EC) in the microvasculature of organs in a process called sequestration. During human *Plasmodium falciparum* infection iRBC are found in organs such as brain, lungs, spleen, placenta, eyes, subcutaneous fat, heart, bone marrow, gut (reviewed by Haldar *et al*., 2007), and more rarely in liver (Whitten *et al*., 2011). Sequestration of *P. falciparum* is associated with the most severe symptoms of human malaria such as cerebral malaria, acute lung injury (ALI), acute respiratory syndrome (ARDS), and pregnancy malaria (Desai *et al*., 2007; Haldar *et al*., 2007).

Other *Plasmodium* species have also been observed in the microvessels of various organs during infection, including those infecting lower primates (Cox-Singh *et al*., 2010), rodents (Smith *et al*., 1982; Gilks *et al*., 1990; Franke-Fayard *et al*., 2005; Amante *et al*., 2010; Claser *et al*., 2011; Fu *et al*., 2012), and more recently *P. vivax* in humans (Anstey *et al*., 2007; Machado Siqueira *et al*., 2012). However, only *P. falciparum* has been found to sequester significantly in the brain, whereas other *Plasmodium* species have been observed mostly in liver, lung and spleen (Weiss *et al*., 1986; Gilks *et al*., 1990; Mota *et al*., 2000; Franke-Fayard *et al*., 2005; Anstey *et al*., 2007; Amante *et al*., 2010; Claser *et al*., 2011; Lacerda *et al*., 2012; Machado Siqueira *et al*., 2012; Manning *et al*., 2012).

In addition to sequestration, inflammatory cytokines, such as IFNγ, TNF and IL1, are also associated with severity of *P. falciparum* and *P. vivax* malaria (Clark *et al*., 2008), as well as *P. berghei*, *P. yoelii* and *P. chabaudi* infections of mice (Stevenson and Riley, 2004; Langhorne

*et al*., 2008). Pro-inflammatory molecules can also induce expression of adhesion molecules, such as E-selectin, ICAM-1 and V-CAM1 on the surface of endothelial cells (Aird, 2007a), which increase and strengthen *in vitro* binding of both *P. falciparum* and *P. vivax* iRBCs (Prudhomme *et al*., 1996; Carvalho *et al*., 2010). It is thus possible that host inflammatory responses influence both pathology and iRBC sequestration *in vivo* during infection.

Sequestration in mouse models has mostly been investigated in depth in *P. berghei* ANKA infections of mice (Lovegrove *et al*., 2008; Amante *et al*., 2010; Baptista *et al*., 2010; Claser *et al*., 2011; Fonager *et al*., 2012; Nacer *et al*., 2012), and to some extent during *P. yoelii* infections (Martin-Jaular *et al*., 2011). Studies of *P. berghei* ANKA have concentrated on sequestration in the brain, often with conflicting results (Franke-Fayard *et al*., 2005; Baptista *et al*., 2010). One limitation of studying sequestration in this model is the asynchronous nature of the erythrocytic cycle. *P. chabaudi*, in contrast, has a synchronous asexual cycle and is the only rodent malaria which demonstrates a defined period of schizont withdrawal from peripheral blood. Parasites have been observed in blood vessels in the liver (Gilks *et al*., 1990; Mota *et al*., 2000). Furthermore the inflammatory response to this infection is well characterized (Freitas do Rosario *et al*., 2012). This infection is thus a very accessible model to examine sequestration, and the influence of parasite-induced inflammation on this process and on malaria pathogenesis.

Here we have carried out a systematic study of sequestration and histopathology of *P. chabaudi* in C57Bl/6 mice. We show that mature stages of *P. chabaudi* accumulate early in infection in the spleen, and later actively sequester in the liver and lungs. Histological changes and host cell damage, observed in multiple organs during a primary blood-stage infection, are similar to those observed in *P. falciparum* and *P. vivax* malaria in humans. The adaptive immune response and IFNγ signalling increase sequestration and histopathological changes specifically in the liver. By contrast an elevated inflammatory response induced in mice lacking IL-10 (Li *et al*., 2003; Sanni *et al*., 2004) increases lung and kidney damage without affecting sequestration in these organs. *Plasmodium chabaudi* therefore provides an excellent model in which to investigate organ-specific pathology and sequestration in malaria.

## Results

### Plasmodium chabaudi *infected erythrocytes sequester in the lungs and liver in a time-dependent manner*

The asexual cycle of *P. chabaudi* in RBC is completed within 24 h and, uniquely among the rodent malarias, is highly synchronous, enabling determination of the timing of sequestration. Analysis of thin blood films over 8 h from trophozoite to schizont maturation, schizogony, and re-invasion of RBC (ring stages) showed that although mature trophozoites were replaced by ring-stage parasites, fewer than 10% of the parasites were schizonts (Fig. 1A and Fig. S1A) indicating that the majority of mature parasites were absent from peripheral blood. There was a consistent decrease of 20–38% in total parasitaemia prior to the appearance of ring-stage parasites (13.00 h), compared with parasitemia at the earlier stages (9.00 h; Fig. 1B, and Fig. S1B).

Analysis of iRBC in blood vessels of lungs, liver, kidney and brain before (9.00 h), during (12.00 h) and after the withdrawal period (17.00 h, Fig. 1C and D) showed that the decrease in peripheral parasitemia was mirrored by a time-dependent increase in iRBC in lungs and liver during schizogony but not in kidney and brain. At 12.00 h, the most significant accumulation of parasites was observed in the liver, 8 days post infection (p.i.) (peak of infection), where up to 90% of blood vessels contained iRBC, and parasitemia inside the microcapillaries was 2–3 times that of peripheral blood (up to 70%). Of interest the accumulation of parasites in the lungs was only observed in the microcapillaries (Fig. 1C and D) where the parasitemia was significantly increased at 12.00 h compared with that observed in the lungs or in the periphery at 9.00 h. Infected RBCs localized within the microcapillaries were abundant in lung, liver and spleen but were rare in kidney and brain. Strikingly, as shown in representative haematoxylin and eosin (H&E) stained tissue sections and electron micrographs (Fig. 1E and Fig. S2B), iRBC were observed lining the endothelium of liver and lungs. These observations together strongly suggest active sequestration in the organs rather than a result of parasite load, or blockage of the microvessels.

To demonstrate sequestration more directly and to investigate its dynamics we examined organs of mice infected with a transgenic line of *P. chabaudi* expressing luciferase (*Pcc*AS*luc*) (Fig. S3A). The course of the *Pcc*AS*luc infection* was similar to that of the wild-type (wt) parasites (Fig. 2A). During schizogony (12.00–14.00 h), *Pcc*AS*luc* was imaged in organs of C57BL/6 mice after intracardiac perfusion (Fig. 2B) from day 5–29 p.i., when a detectable parasite recrudescence was observed.

Infected RBCs were predominantly in the spleen early in infection. However, because of the nature of the splenic architecture, perfusion of the spleen is not efficient (Fig. S2A), therefore it was not possible to differentiate between sequestration and accumulation in this organ. By contrast, sequestration could clearly be measured in lungs and liver where perfusion was very effective, and, these were the dominant sites of sequestration by day 8

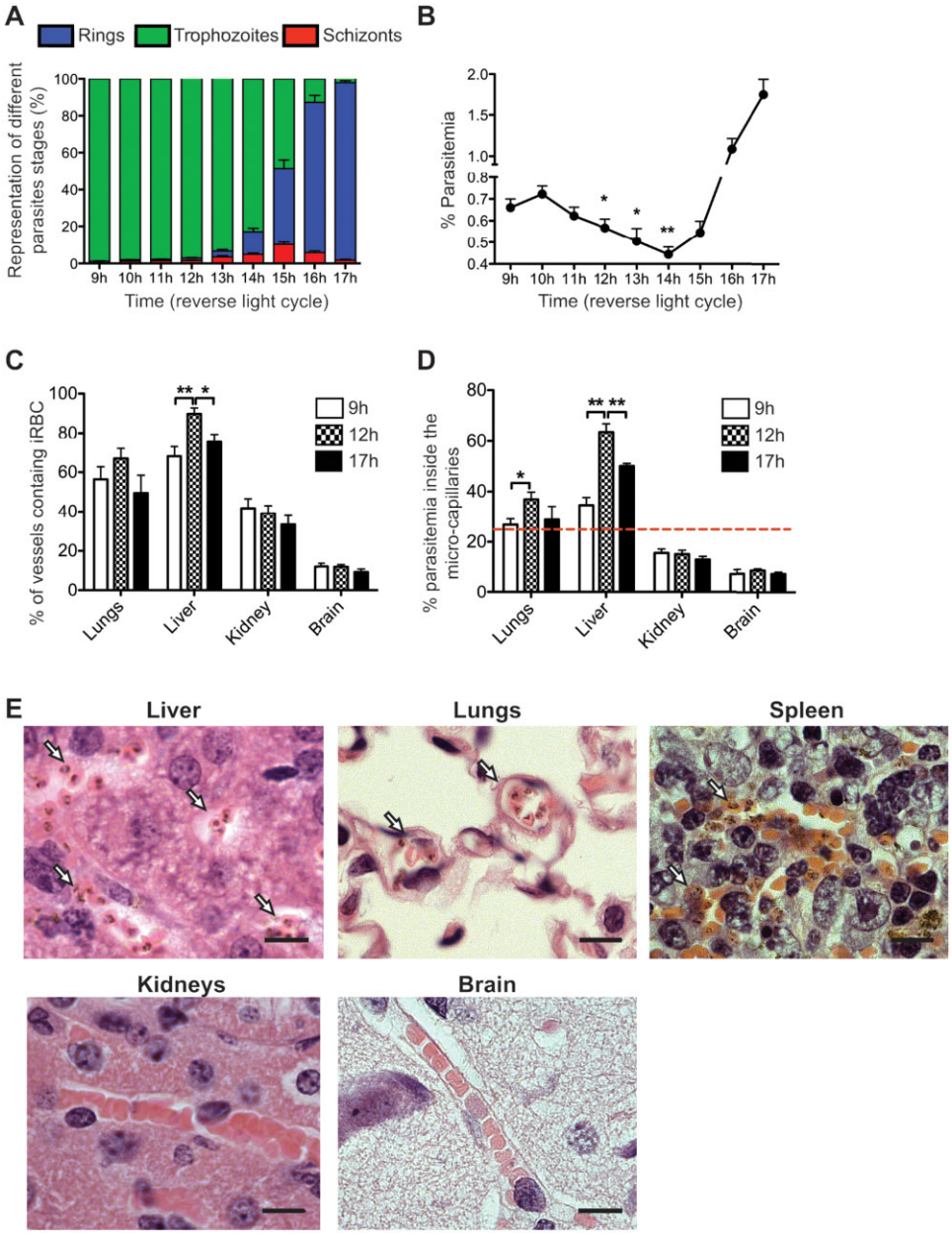


**Fig. 1.** Mature stages of *Plasmodium chabaudi* leave the peripheral circulation and accumulate in organs. C57BL/6 mice were maintained in a reverse 12 h light–dark cycle and infected with $10^5$ wild type *P. chabaudi* iRBC. Tail blood was taken hourly between 9 h and 17 h, on day 5 of infection.
A. Stages of the parasite life cycle observed in peripheral blood.
B. parasitemia in peripheral blood. Parasitemias at each time point were compared with parasitemia at 9.00 h.
C. Percentage of microvessels in different organs containing *P. chabaudi* iRBC. 200 vessels were counted for each organ on H&E stained sections (see *Experimental procedures*).
D. percentage of RBC infected within the microvessels of the different organs. 400 RBC were counted on each section for each organ on every sample. The red dotted line indicates the average peripheral parasitemia at 9.00 h.
E. Representative tissue sections made at 12.00 h, 8 days after infection and stained by H&E. Infected red blood cells are indicated by arrows. Scale bars represent 10 μm. Each dot or bar represents the average for at least 8 mice (± SEM) (*$P < 0.05$; **$P < 0.01$; ***$P < 0.001$, Mann–Whitney test).

(Fig. 2C). Interestingly, maximum sequestration in lungs and liver occurred at day 9, when there is a significant host response (Stevenson and Riley, 2004; Freitas do Rosario *et al.*, 2012), and numbers of iRBC in the blood had declined dramatically (Fig. 2C). It is also important to note that the level of sequestration decreases rapidly in the liver after day 9 while it remains relatively high in the lungs until day 13 indicating that the molecules implicated

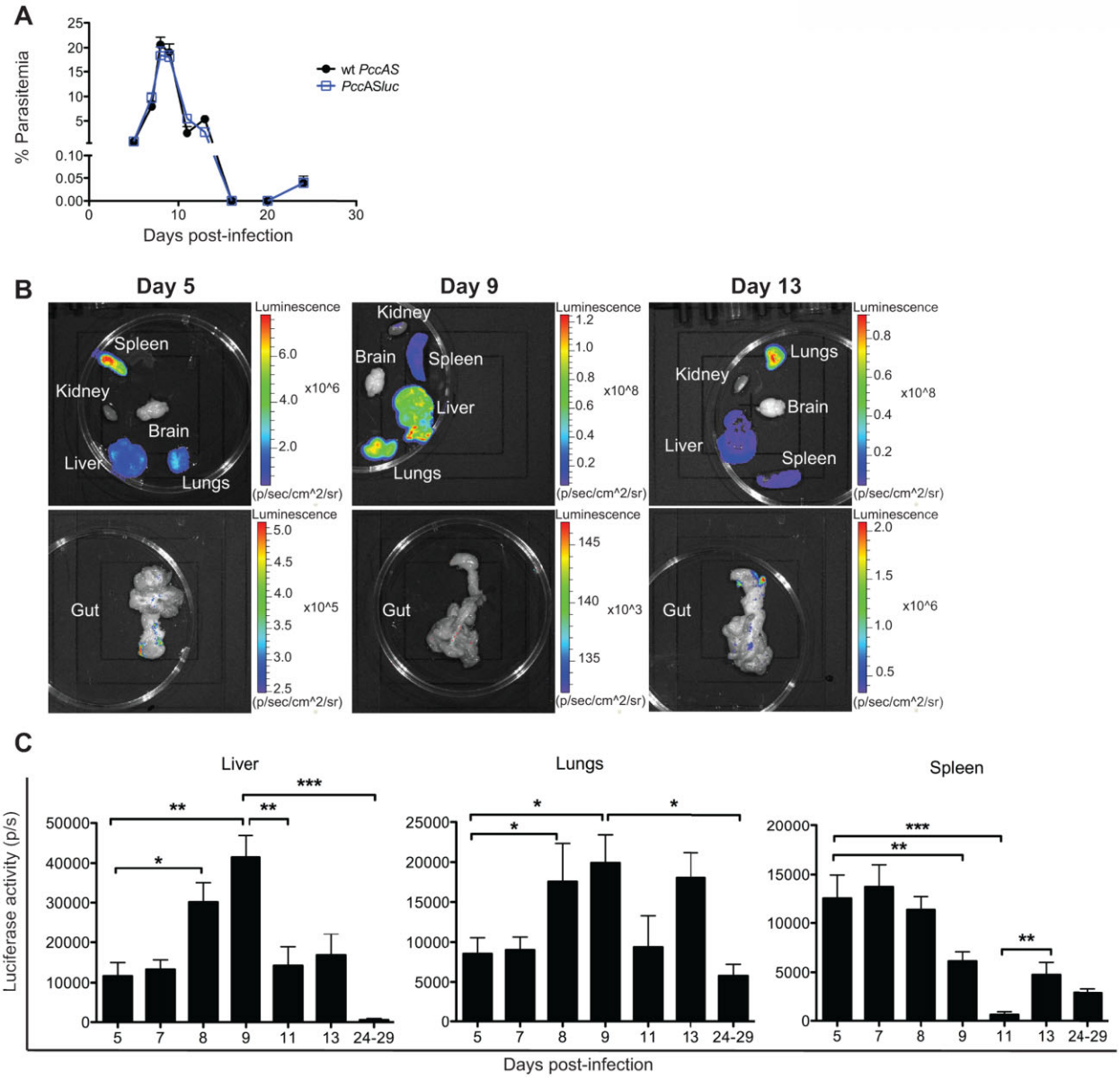


**Fig. 2.** *Plasmodium chabaudi* sequester preferentially in lungs, liver and spleen in a time-dependent manner.
A. Parasitemia in mice infected with $10^5$ wild-type C57BL/6 mice and luciferase-expressing *P. chabaudi* (*PccASluc*) infected RBC. Luciferase activity in organs was measured between 12.00 h and 14.00 h after whole body perfusion.
B. Representative images of *PccASluc* accumulation in extracted organs.
C. The luciferase activity (p/s) measured in each organ was normalized as described in *Experimental procedures*. Each bar represents the average for ten mice (± SEM). (*$P < 0.05$; **$P < 0.01$; ***$P < 0.001$, Mann–Whitney test).

in *Pcc* AS sequestration are different and/or differentially regulated in these two organs. Only a low level of sequestration was observed in the gut, but luciferase activity could be detected in the surrounding visceral fat tissue (data not shown). Similar to the histological findings, at no time point was sequestration observed in brain or kidney (data not shown).

### *The adaptive immune response and IFNγ influence sequestration in the liver but not lung during* P. chabaudi *infection*

A *P. chabaudi* blood-stage infection in C57BL/6 mice induces an immune response characterized by pro-inflammatory cytokines such as TNF and CD4 T-cell

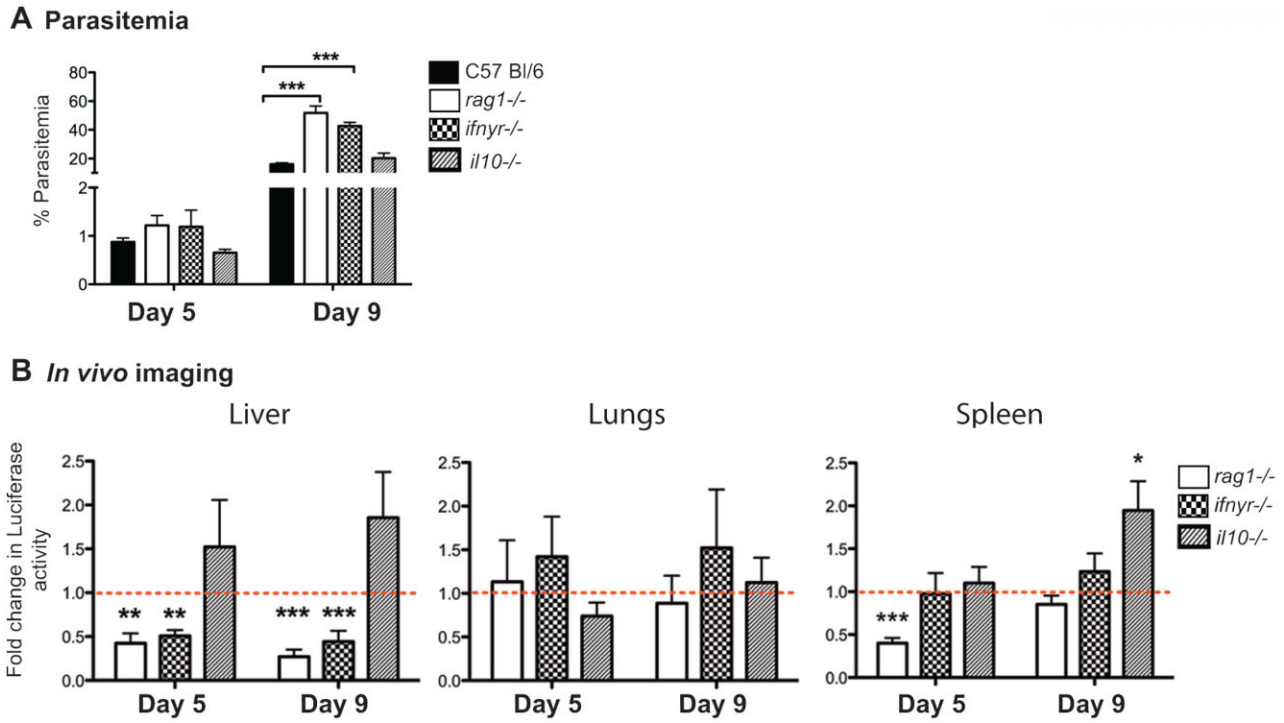


**Fig. 3.** Adaptive immune responses and IFNγ response increase sequestration in the liver during *Plasmodium chabaudi* infection. Wild type (wt) C57BL/6 mice and mice lacking an adaptive immune system (*rag1*$^{-/-}$) IFNγ receptor (*ifnγr*$^{-/-}$) or IL-10 (*il10*$^{-/-}$) were infected with $10^5$ luciferase-expressing *P. chabaudi* iRBC (*PccASluc*).
A. Comparison of peripheral parasitemia in the different strains of mice on days 5 and 9 of infection measured at 9.00 h.
B. Luciferase activity in liver, lungs and spleen of infected *rag1*$^{-/-}$, *ifngr*$^{-/-}$ and *il10*$^{-/-}$ mice expressed as fold change relative to luciferase activity in wt C57BL/6 mice measured after whole body perfusion at days 5 and 9 post infection. Each bar represents the average for at least six mice (± SEM). (*$P < 0.05$; **$P < 0.01$; ***$P < 0.001$, Mann–Whitney test).

derived IFNγ. IL10 is a crucial regulator of this pro-inflammatory response (Li *et al.*, 2003; Sanni *et al.*, 2004; Freitas do Rosario *et al.*, 2012). Pro-inflammatory cytokines can induce or increase expression of some adhesion molecules on the surface of EC (Aird, 2007a), and they influence adhesion of iRBCs to ECs *in vitro* (Prudhomme *et al.*, 1996; Mota *et al.*, 2000; Carvalho *et al.*, 2010). We therefore asked whether the adaptive immune response and inflammatory cytokines would affect *P. chabaudi* sequestration *in vivo* using mice lacking T and B cells (*rag1*$^{-/-}$), the IFNγ receptor (*ifnγr*$^{-/-}$ *mice*), or IL-10 (*il10*$^{-/-}$.) As the major differences in sequestration patterns were seen between days 5 and 9 p.i. in C57BL/6 mice, those time points were chosen for further analysis.

*Plasmodium chabaudi* iRBCs were still present after perfusion of the organs of *rag1*$^{-/-}$ mice (Fig. 3B) indicating that adaptive immunity was not required for sequestration. However there was a significant reduction of iRBC sequestration at day 5 (prior to peak infection), and day 9 (1 day post peak infection) in the livers of *rag1*$^{-/-}$ mice and *ifnγr*$^{-/-}$ mice, despite higher peripheral parasitemias (Fig. 3A and B). By contrast, deletion of either gene had no effect on sequestration in the lung (Fig. 3B).

The lack of IL10 did not affect overall peripheral parasitemia (Fig. 3A and Li *et al.*, 2003). However there was a significantly greater withdrawal of iRBC from the periphery (Fig. S1D, and Sanni *et al.*, 2004), and, although not statistically significant, the level of sequestration in the liver was, on average, two fold higher in *il10*$^{-/-}$ mice than in C57BL/6 wt mice (Fig. 3B). The lack of IL10 did not affect sequestration of iRBC in the lungs, which remained at the level of wt mice (Fig. 3B). The accumulation of iRBC in the spleen of *il10*$^{-/-}$ mice was significantly higher at day 9 compared with wt C57BL/6 mice and *rag*$^{-/-}$ and *ifnγr*$^{-/-}$ mice. As it was not possible to differentiate between sequestration and accumulation in this organ, the mechanisms underlying these differences are as yet unknown.

Despite the presence of oedema and haemorrhages previously observed in brains of *il10*$^{-/-}$ mice (Sanni *et al.*, 2004), there was no observable sequestration of iRBC in this organ (data not shown), suggesting that the pathology associated with the brain is mediated by an inflammatory response.

The effects of the adaptive immune response and pro-inflammatory responses therefore enhance sequestration of *P. chabaudi* in the liver but not in the lung.

### Plasmodium chabaudi *infection induces histopathological changes in multiple organs*

Histological analysis of brain, lung, liver and kidney was performed throughout the course of the *P. chabaudi* blood-stage infection in C57BL/6 mice (Fig. 4).

Extramedullary haematopoesis (EMH) and greater numbers of Kuppfer cells were observed in the liver between day 5 and 13 of infection with focal necrosis at peak infection (Fig. 4A). Hepatocellular degeneration and necrosis was indicated by increase in the level of the liver enzyme alanine transaminase (ALT) in plasma on days 8 and 9.

Changes in the lung were observed during acute infection with increased cellularity of the alveolar septae from day 7 to 13 p.i. (Fig. 4B). Flow cytometric analysis showed a significant increase in the number of dendritic cells ($CD11c^+$, $MHCII^{high}$), monocytes ($Ly6C^{high}$, $CD11b^+$, $Ly6G^-$), neutrophils ($Ly6G^+$, $CD11b^+$, $Ly6C^{int}$) and $CD8^+$ T cells, but not CD4 T cells or macrophages ($CD11c^+$, $CD11b^{low/-}$, $F4/80^{int}$, $MHCII^+$) in lung tissue (Fig. S4). There were also elevated numbers of IFNγ-producing lymphocytes (Fig. 4B). Of the IFNγ-producing cells, 60% were $CD3^+CD90.2^+$, among which 50% were $CD4^+$ and 20% were $CD8^+$ T cells (data not shown). There was a significant increase in the amount of IgM in the BAL (Fig. 4B) indicating some disruption of the alveolar-capillary membrane barrier (Lovegrove *et al*., 2008) at Day 8, and during the resolution of infection (Day 13).

Tubular dilatation was observed throughout the infection in the kidney showing that *P. chabaudi* infection induced histopathological changes even in the absence of sequestration (Fig. 4C). However, no significant differences of urea and creatinine levels in serum were observed between infected and uninfected animals at any stage of infection, suggesting no major impairment of kidney function in infected C57Bl/6 mice. There were no observable changes in the brain.

In summary, histopathological changes were observed in liver and lung where sequestration takes place, and some minor changes in the kidney where no sequestration was observed.

### *Pro-inflammatory responses increase histopathological changes in an organ-specific manner during* Plasmodium chabaudi *infection*

As we had observed that the adaptive response, and pro-inflammatory responses affected sequestration in liver but not lungs, we also asked whether these responses affected any of the *P. chabaudi*-associated histopathology observed.

In line with the reduction in sequestration described above, hepatocyte damage, as determined by ALT in plasma was significantly reduced in infected *rag1*$^{-/-}$ mice and *ifnγr*$^{-/-}$ mice compared with infected wt mice (Fig. 5A). By contrast, the increased ALT levels in *il10*$^{-/-}$ mice were comparable with those of wt mice (Fig. 5A).

As would be expected, there were few infiltrating cells in the lungs of *rag1*$^{-/-}$ mice (Fig. S4B) and few IFNγ producing cells compared with wt mice (data not shown), whereas the numbers of these cells were unaltered by the lack of the IFNγ receptor (Fig. 5B). In line with a general increase in the inflammatory response in *il10*$^{-/-}$ mice (Freitas do Rosario *et al*., 2012), there were alterations in the populations of infiltrating cells and greater numbers of IFNγ-producing cells in the lungs (Fig. 5B and Fig. S4B) compared with wt mice.

Despite the fact that sequestration was unaltered in the lungs of all of the immunodeficient mice, there was significantly more IgM in the BAL of *il10*$^{-/-}$ mice compared with infected wt mice (Fig. 5B). Surprisingly there was no change in the amount of IgM in BAL of *ifnγr*$^{-/-}$ compared with their wt controls, suggesting that IFNγ signalling was

**Fig. 4.** Histopathological changes in organs during *Plasmodium chabaudi* infection.
C57BL/6 mice were infected with $10^5$ wild-type *P. chabaudi* iRBC. Representative H&E sections from liver, lung and kidney of uninfected (control) or infected mice (day 8 p.i.) are shown.
A. Liver: upper panel shows extramedullary haematopoiesis (EMH) (1) and pigmented kupfer cells (2); lower panel shows a region of focal necrosis (indicated within the marked area). Scale bars represent 100 μm. The upper right graph is a semi-quantitative measure of EMH, Kupffer cells and necrosis using the scoring system described in *Experimental procedures*. The lower right graph shows the increase in alanine transaminase (ALT) in plasma during infection as an indication of liver damage.
B. Lung: upper left panel shows increased alveolar septae cellularity; upper right graph shows the enumeration of this cellularity using the scoring system described in *Experimental procedures*; lower left graph shows the number of IFNγ-producing lymphocytes in the lung of uninfected mice and mice infected with *P. chabaudi* for 5, 8 and 13 days. Lower right graph shows the increase in IgM in the BAL of *P. chabaudi* infected mice, as measured by ELISA.
C. Kidney: left panels show tubular dilatation; right upper graph show a semi-quantitative measure of tubular dilatation using the scoring system described in *Experimental procedures*; lower graphs shows the amounts of creatinine and urea in plasma of uninfected and *P. chabaudi* infected mice at days 5, 8, 9 and 13. Each bar represents the average for at least five mice (± SEM). (*$P < 0.05$; **$P < 0.01$; ***$P < 0.001$, Mann–Whitney test).

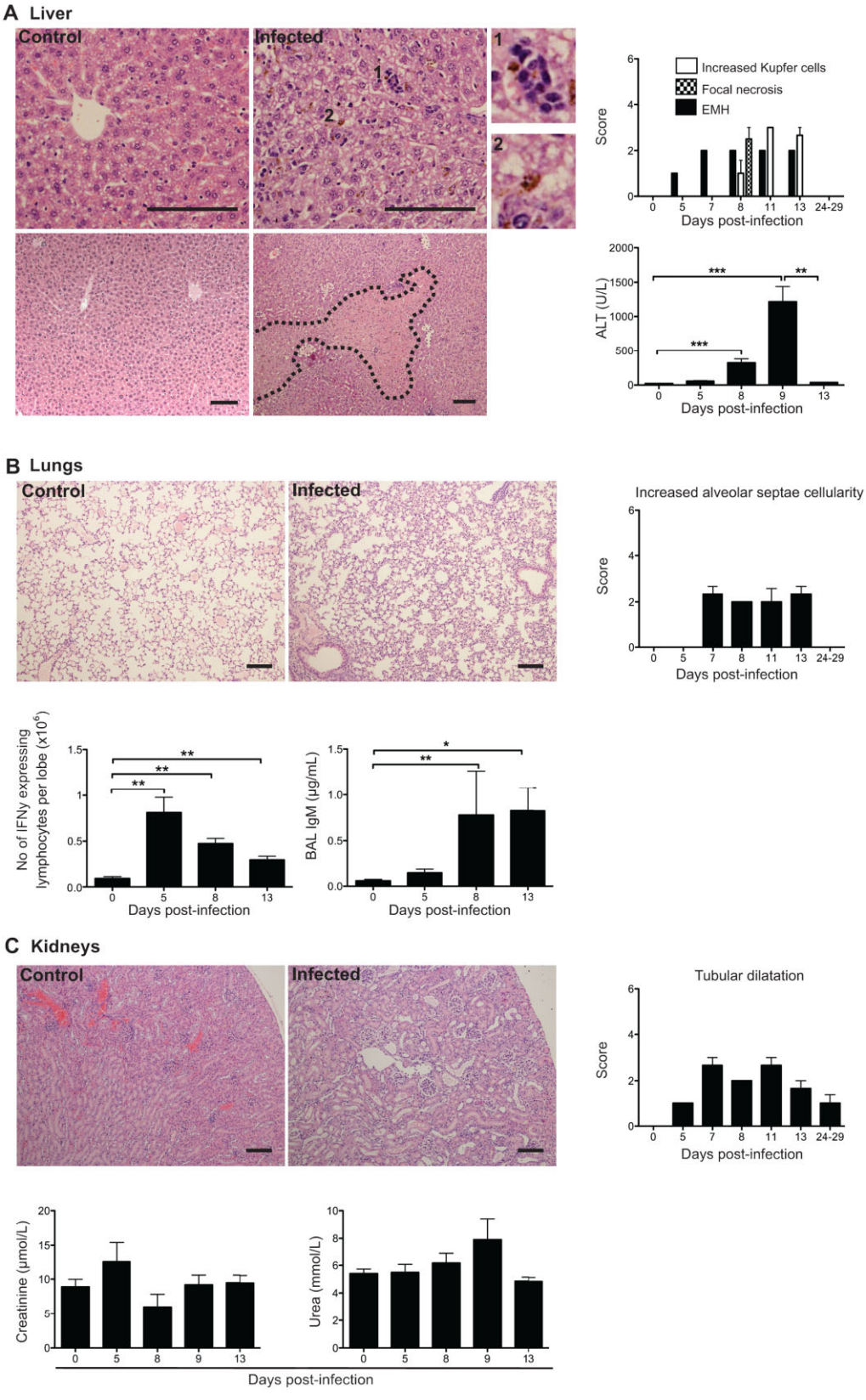

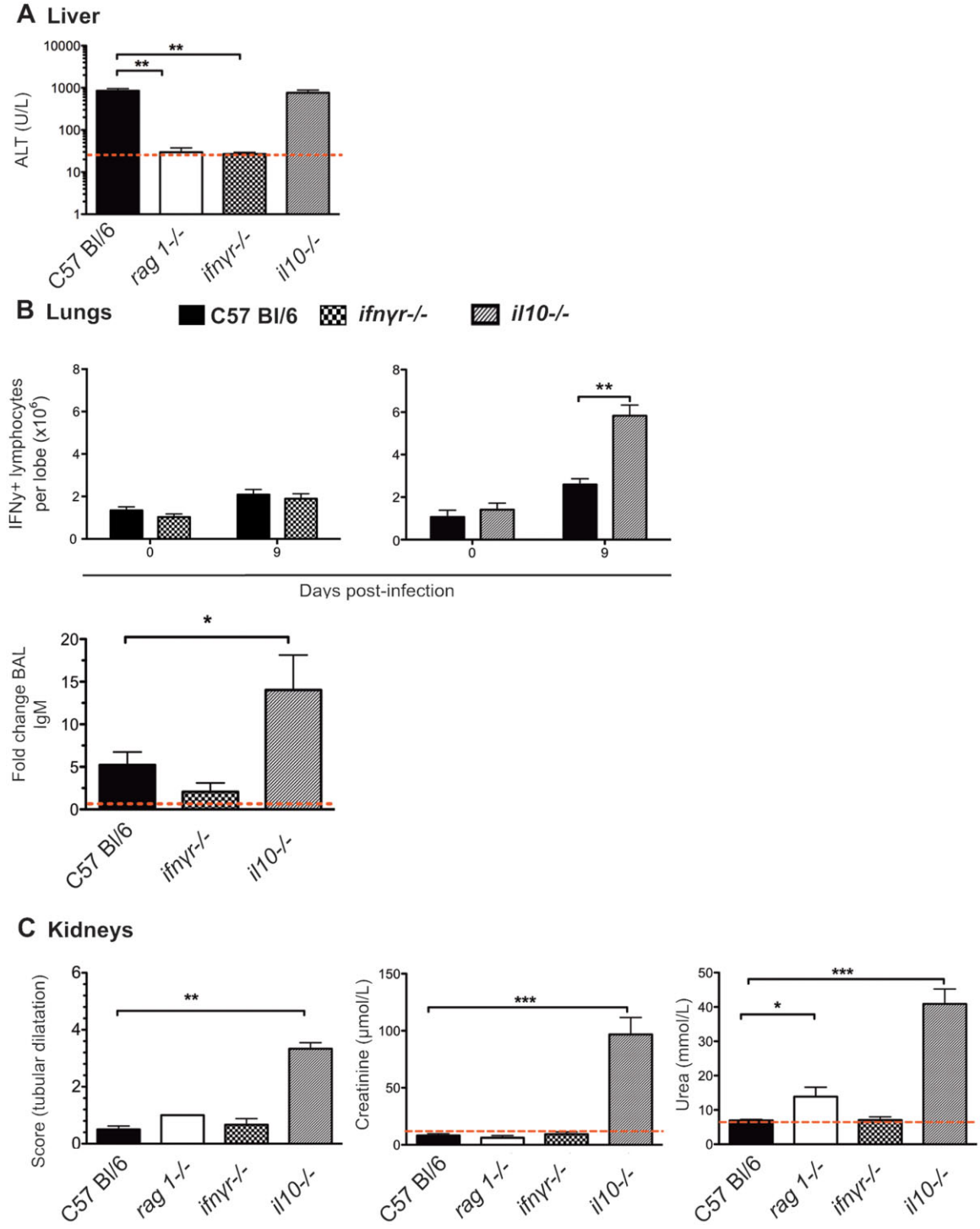


**Fig. 5.** Pro-inflammatory response increases damage in multiple organs during *Plasmodium chabaudi* infection. Wild type (wt) C57BL/6 mice and mice lacking an adaptive immune system (*rag1*$^{-/-}$) IFNγ receptor (*ifnγr*$^{-/-}$) or IL-10 (*il10*$^{-/-}$) were infected with $10^5$ wild-type *P. chabaudi* iRBC.

A. Liver: increase in alanine transaminase (ALT) in plasma during infection as an indication of liver damage.

B. Lung: upper panels show the number of IFNγ-producing lymphocytes in the lung of uninfected mice and mice infected with *P. chabaudi* for 9 days. Lower graph shows the increase in IgM in the BAL of *P. chabaudi* infected mice (measured by ELISA) expressed as fold change relative to uninfected mice of the same genetic background (indicated by the dotted line).

C. Kidney: left panel show a semi-quantitative measure of tubular dilatation using the scoring system described in *Experimental procedures*; middle and right graphs shows the amounts of creatinine and urea in plasma of *P. chabaudi* infected mice at days 9. Each bar represents the average for at least five mice (± SEM). (*$P < 0.05$; **$P < 0.01$; ***$P < 0.001$, Mann–Whitney test).

not involved in alveolar-capillary membrane barrier disruption. As *rag1*$^{-/-}$ mice do not produce immunoglobulin it was not possible to use BAL IgM as an indicator of damage to the alveolar-capillary membrane barrier in these mice. Measurement of BAL albumin was similar in wt, *ifnγr*$^{-/-}$ and *rag*$^{-/-}$ mice (Fig. S4C) but, consistent with the measurement of IgM, was slightly elevated in infected *il10*$^{-/-}$ mice.

There was no significant change in kidney histopathology in *ifnγr*$^{-/-}$ mice, and only a small increase in urea in *rag1*$^{-/-}$ mice. However, in *il-10*$^{-/-}$ mice there was clearly more tubular dilatation and significantly elevated urea and creatinine in the plasma, indicating increased kidney damage and loss of function (Fig. 5C).

Adaptive immunity and IFNγ therefore contribute to liver damage, but not to the disruption of alveolar-capillary membrane barrier of the lung, or to damage of any of the other organs examined. The acute lung and kidney injury observed in *P. chabaudi* infections appear to be independent of adaptive immunity, IFNγ and the amount of parasite sequestration or burden, but are associated with the greater inflammatory response of *il10*$^{-/-}$ mice.

## Discussion

We have investigated parasite sequestration and histopathological changes occurring in C57BL/6 mice during an infection with the rodent malaria parasite, *Plasmodium chabaudi*, and show that adaptive immunity and an inflammatory response increase sequestration of *P. chabaudi* iRBC, and contribute to pathology in an organ-specific manner.

We show, for the first time, sequestration of *P. chabaudi* iRBC in the lungs during infection and, in agreement with previous histological studies (Cox *et al*., 1987; Gilks *et al*., 1990; Mota *et al*., 2000), demonstrate sequestration in the liver. However no significant sequestration could be observed in kidneys, brain or gut. Although there was not a complete lack of schizonts in peripheral blood, similar to observations of *P. vivax* infections in humans (Field and Shute, 1956), parasitemia in the microvessels of the lungs and liver was significantly greater than that in peripheral blood during schizogony, and parasites were observed lining the endothelium, strongly supportive of active sequestration in these organs.

There are similarities in this sequestration pattern with other rodent malaria species. *Plasmodium berghei* ANKA iRBCs are found in the lungs, liver, spleen and visceral fat tissue, but substantially fewer in the brain (Franke-Fayard *et al*., 2005; Amante *et al*., 2010; Fonager *et al*., 2012). *P. yoelii* has been shown by histology to accumulate in the spleen, liver, brain and kidney (Smith *et al*., 1982; Fu *et al*., 2012), but a comparison between organs has not yet been performed. The relative lack of sequestration of the rodent malaria parasites in the brain, but their accumulation in the liver, spleen and lungs is more similar to that described so far for the human infection with *P. vivax* (De Brito *et al*., 1969; Anstey *et al*., 2007; Machado Siqueira *et al*., 2012; Manning *et al*., 2012).

Sequestration is mediated by adhesion of parasite proteins expressed on iRBC to EC receptors (reviewed by Rowe *et al*., 2009). The human parasite *P. vivax* and rodent malarias lack the *var* multigene family (Cunningham *et al*., 2010), which is implicated in sequestration of *P. falciparum* and associated with cerebral malaria (Rowe *et al*., 2009; Avril *et al*., 2012; Claessens *et al*., 2012). This may be one explanation why, unlike *P. falciparum*, *P. chabaudi* and *P. vivax* do not accumulate in the brain. Although neither the parasite nor the host adhesion molecules involved in its sequestration are known, *P. chabaudi* shares several analogous multigene families coding for potential parasite adhesion molecules with high similarity to genes of *P. vivax* (e.g. *pir* genes) (Cunningham *et al*., 2010; Lawton *et al*., 2012). It has been shown *in vitro* that expression of *pir* genes from *P. vivax* in *P. falciparum* iRBC enhanced their adhesion to EC receptors such as ICAM-1 (Bernabeu *et al*., 2012). As *P. vivax* and rodent malaria parasites share this multigene family it is possible that they have a similar potential for cytoadherence by the same host receptors and, thus, explain why they sequester within the same organs.

Histopathological changes occur in several organs during human malaria, some of which are in the organs where iRBC sequestered. Acute lung injury characterized by thickened alveolar septa and intra-alveolar haemorrhages, liver damage associated with Kupffer cell hyperplasia, necrosis and an increase of plasma ALT and bilirubin levels, and kidney failure associated with tubular haemoglobin casts and increased serum creatinine and urea levels are common complications during both *P. vivax* and *P. falciparum* infection (Haldar *et al*., 2007; Anstey *et al*., 2009). During *P. chabaudi* infection, we observed similar changes in liver and lung coincident with sequestration such as liver necrosis, with elevated plasma ALT level, and inflammatory cell infiltration in the lung and presence of IgM in the BAL consistent with alveolar-capillary membrane barrier disruption (Lovegrove *et al*., 2008). We also observed tubular dilatation in the kidney, where no sequestration was observed. The finding of sequestered parasites and tissue damage in the lungs is similar to that described for both *P. falciparum* and *P. vivax* (Anstey *et al*., 2007; Lacerda *et al*., 2012), and respiratory distress syndromes have been described in all five malaria species infecting humans (reviewed by Taylor *et al*., 2004). The *P. chabaudi* experimental model system may therefore facilitate the further investigation of the relationship between sequestered parasites and respiratory clinical syndromes.

The host immune response and particularly pro-inflammatory cytokines can potentially influence both sequestration and pathological sequelae of malaria. *In vitro*, TNF and IFNγ upregulate expression of endothelial adhesion molecules such as I-CAM, V-CAM, P- and E-selectin (Aird, 2007a), and increase the binding of RBC infected by *P. falciparum*, *P. vivax* or *P. chabaudi* to endothelium *in vitro* (Prudhomme *et al*., 1996; Mota *et al*., 2000; Carvalho *et al*., 2010). Here we demonstrate that T and B cells and signalling through the IFNγ receptor enhance sequestration of *P. chabaudi* in the liver but not the lung.

The expression of adhesion molecules on endothelial cells, such as VCAM-1 and ICAM-1, differs both constitutively and after activation in organs such as brain, spleen and lung (Oh *et al*., 2004; Aird, 2007a,b). Furthermore, P- and E-Selectins, which are highly upregulated in the brain and implicated in cerebral malaria during *P. berghei* infection, are not expressed on endothelial cells from liver sinusoids (Combes *et al*., 2004; Aird, 2007a,b). In mice lacking T and B cells or the IFNγ receptor, we observed changes in sequestration only in the liver but not in the spleen or lungs, suggesting that *P. chabaudi* may use more than one endothelial cell receptor for adhesion, the expression of which may be inducible to different levels in these organs. It is also possible that different populations of iRBC sequester in these organs with different parasite ligands. These possibilities are currently under investigation.

Alteration in inflammatory cytokines also affected the pathological changes observed during *Plasmodium chabaudi* infection but differently in the different organs. The lack of the IFNγ receptor and T and B cells resulted in a reduction not only in liver sequestration but also lower ALT levels in the plasma, despite a higher parasitemia. In *il10*$^{-/-}$ mice with an exacerbated inflammatory response to *P. chabaudi* infection (Sanni *et al*., 2004; Freitas do Rosario *et al*., 2012), there was increased IgM and albumin in the BAL indicating disruption of the alveolar-capillary membrane barrier, despite no change in parasitemia or amount of sequestration in the lungs. Kidney damage was also observed in these mice without any significant parasite sequestration. Similarly, there was no sequestration in the brain, where oedema and haemorrhages have been described in *P. chabaudi* infected *il10*$^{-/-}$ mice (Sanni *et al*., 2004).

Our results demonstrate that adaptive immunity and inflammatory responses affect sequestration and histopathology in an organ-specific manner. To understand fully the pathogenesis of human malaria and the host/pathogen interactions taking place during this infection, it will therefore be necessary to dissect these mechanisms in all organs of interest. *P. chabaudi* is a good model in which to dissect these mechanisms, which may be directly relevant for aspects of both *P. falciparum*- and *P. vivax* associated disease.

## Experimental procedures

### *Ethics statement*

This study was carried out in accordance with the UK Animals (Scientific Procedures) Act 1986 (Home Office licence 80/2538), and was approved by the National Institute for Medical Research Ethical Committee. All surgery was performed under sodium pentobarbital anaesthesia, and all efforts were made to minimize suffering.

### *Mice*

Female C57BL/6 and BALB/c, B6.*rag1*$^{-/-}$ (Mombaerts *et al*., 1992), B6.*ifnγr*$^{-/-}$ (Huang *et al*., 1993), B6.*il10*$^{-/-}$ (Kuhn *et al*., 1993) aged 6–8 weeks from the SPF unit at the MRC National Institute for Medical Research were housed conventionally with sterile bedding, food and irradiated water on a reverse 12 h light–dark cycle.

### *Parasites*

A transgenic line of *Plasmodium chabaudi chabaudi* (AS) expressing luciferase (*Pcc*AS*luc*) under the control of the constitutive promoter EF1α was generated by transfection with the plasmid pPc-LUC$_{CAM}$ targeting the small subunit ribosomal RNA locus and the insertion was verified by Southern blot analysis as described (Spence *et al*., 2011) (Fig. S3A). For all other experiments, a cloned line of wild type *P. chabaudi* AS strain was used in this study. Infections were initiated by intraperitoneal (i.p.) injection of $10^5$ iRBC, and monitored by examination of Giemsa-stained blood films. *Pcc*AS*luc* parasites were maintained in mice given acidified water containing pyrimethamine to select for transfected parasites (Spence *et al*., 2011).

### *Histology*

Mice were euthanized by i.p. injection of pentoject (Animal Care), the trachea was cannulated and lungs inflated by injection of 3 ml of 4% M/V formaldehyde (VWR). The brain, left lobes of the lung and liver, left kidney and spleen from infected and uninfected mice were fixed in 4% VWR for 24 h at room temperature. Fixed organs were embedded in wax, sectioned (5 μm), and stained with H&E. Sections were examined microscopically and changes recorded using a standard non-linear semi-quantitative scoring system using a scale from 0 to 5 adapted from Shackelford *et al*. (2002) (Scudamore, in press). Significant findings were scored 0 (where no change was detectable), 1 when the least amount of change was detectable by light microscopy (usually < 10% of tissue affected), 2 when change was readily detected but not a major feature (< 20%), 3 when the change was more extensive and might be expected to correlate with changes in organ weight or function, 4 when up to 75% of tissue was affected by the change and 5 when the whole tissue was affected by a change which was likely to be functionally relevant. Organs from infected mice were always compared with those from uninfected controls

on the same day. The percentage of vessels in each organ containing iRBC was determined from 400 vessels, and the percentage parasitemia in the vessels was counted in a minimum of 200 RBC.

### In vivo *imaging and luciferase assay*

At selected times after infection with *Pcc*AS*luc*, at maximum sequestration (12.00 h to 14.00 h, reverse light, Fig. 1), D-luciferin (150 mg $kg^{-1}$, Caliper Life Sciences) was injected subcutaneously 5 min before imaging. Mice were terminally anaesthetized and perfused by intracardiac injection of PBS (Fig. S2A). The brain, lungs, liver, spleen, left kidney and gut were removed immediately and luciferase was assessed using *in vivo* Imaging System IVIS Lumina (Xenogen), with a 10 cm field of view, a binning factor of 4, and an exposure time of 10 s. Bioluminescence (p/s) was quantified with the software Living Image (Xenogen) by adjusting a region of interest to the shape of each organ.

To account for the influence of total parasite load on the number of parasites sequestered in the organs, bioluminescence in the organs was normalized to total parasite load. Because of the dark pigmentation of C57BL/6 mice, measurement of parasite burden by whole body imaging was not accurate (Fig. S3B). For each mouse, 2 μl of heparinized tail blood was collected before sequestration (9.00 h). Bioluminescence was assessed with the Luciferase Assay System (Promega) according to the manufacturer's protocol and quantified with the TECAN Safire2 plate reader and Magellan software (Tecan). Under these conditions, bioluminescence intensity is proportional to the amount of parasites in this blood volume (Fig. S3C). This value was taken to reflect parasite burden in the whole body. Luciferase activities measured in the organs were normalized to this value, allowing comparison between mice with different parasite burdens.

### *Alanine transaminase, urea and creatinine quantification in the plasma*

Alanine transaminase, urea and creatinine were quantified in plasma from blood obtained by cardiac puncture under terminal anaesthesia using a Cobas C111 chemistry analyser (Roche).

### *Bronchoalveolar lavage fluids (BAL) analysis*

Uninfected and infected mice were euthanized by intraperitoneal injection of pentoject (Animal Care). The trachea was cannulated and bronchoalveolar lavage (BAL) performed using 1 ml of PBS (Gibco/Invitrogen). BALs were centrifuged at 900 *g* for 5 min at 4°C. IgM and albumin in BAL were measured by sandwich ELISAs (IgM, eBioscience, San Diego CA; albumin, Genway San Diego, CA).

### *Flow cytometric analysis*

After BAL, lung tissue was dissected, minced, incubated in Liberase (40 μg $ml^{-1}$; Roche Diagnostics) at 37°C for 1 h and disrupted by subsequent passage through a 70 μm nylon cell strainer (BD Bioscience). Cells were counted, and diluted in Iscove's modified Dulbecco's medium (Sigma) supplemented with 10% FBS (PAA), 0.05 mM β-mercaptoethanol (Gibco), 2 mM L-glutamine (Gibco), 0.5 mM sodium pyruvate (Sigma), 6 mM Hepes (Gibco), 100 U $ml^{-1}$ penicillin and 100 μg $ml^{-1}$ streptomycin (Gibco). For flow cytometry, single-cell suspensions were incubated with FcR block (BD Bioscience) followed by specific Abs: CD4-V500 (BD Bioscience), Ly6G-PE (Biolegend), MHCII-FITC (Biolegend), 7AAD-PerCP (eBiosciences), Ly6G -V500 (Biolegend), CD90.2-APC (Biolegend), CD11c-APC-Cy7 (Biolegend), CD11b-PacificBlue (eBiosciences), F4/80-PE -Cy7 (Biolegend), CD19-APC-Cy7 (Biolegend), CD3-PE-Cy7 (Biolegend). After surface labelling, cells were fixed with 2% paraformaldehyde in PBS, and permeabilized with Cytofix/ CytopermTM (BD Biosciences). Intracellular IFNγ was detected using IFNγ-PE (Biolegend) as described (Freitas do Rosario *et al*., 2012). Samples were acquired on a FacsCanto II® (BD Bioscience) using Summit Cytomation FlowJo (Tree Star, Inc.) software for analysis.

### *Transmission electron microscopy*

Mice were terminally anaesthetized and perfused by intracardiac injection of PBS. Samples were immersion fixed in 2% glutaraldehyde/2% paraformaldehyde and post fixed in 1% osmium tetroxide using 0.1 M sodium cacodylate buffer pH 7.2. Aqueous uranyl acetate was followed by dehydration through a graded ethanol series, propylene oxide and embedding was in Epon, 50 nm sections were mounted on pioloform coated grids and stained with ethanolic uranyl acetate followed by Reynold's lead citrate. They were viewed with Gatan Orius 1000 CCD.

### *Statistics*

Data are shown as means and SEM. The non-parametric Mann–Whitney *U* test was used and *P* values below 0.05 were considered as statistically significant.

## Acknowledgements

We would like to thank NIMR Biological Services, the Flow Cytometry facilities, Radma Mahmood of the Histology facilities and Liz Hirst of the Electron Microscopy facilities for their skilled technical assistance. This work was supported by the Medical Research Council, UK (U117584248); Singapore A*Star-UK MRC collaborative grant (A*Star reference 10/1/22/24/630), and received funding from the European Union Seventh Framework Programme (FP7/2007-2013) under grant agreement no. 242095-EVIMalaR. P.J.S is the recipient of a Leverhulme Trust early career fellowship.

## Conflict of interest disclosures

The authors declare that they have no competing interests.

## References

Aird, W.C. (2007a) Phenotypic heterogeneity of the endothelium: I. Structure, function, and mechanisms. *Circ Res* **100:** 158–173.

Aird, W.C. (2007b) Phenotypic heterogeneity of the endothelium: II. Representative vascular beds. *Circ Res* **100:** 174–190.

Amante, F.H., Haque, A., Stanley, A.C., Rivera Fde, L., Randall, L.M., Wilson, Y.A., *et al*. (2010) Immune-mediated mechanisms of parasite tissue sequestration during experimental cerebral malaria. *J Immunol* **185:** 3632–3642.

Anstey, N.M., Handojo, T., Pain, M.C., Kenangalem, E., Tjitra, E., Price, R.N., and Maguire, G.P. (2007) Lung injury in vivax malaria: pathophysiological evidence for pulmonary vascular sequestration and posttreatment alveolar-capillary inflammation. *J Infect Dis* **195:** 589–596.

Anstey, N.M., Russell, B., Yeo, T.W., and Price, R.N. (2009) The pathophysiology of vivax malaria. *Trends Parasitol* **25:** 220–227.

Avril, M., Tripathi, A.K., Brazier, A.J., Andisi, C., Janes, J.H., Soma, V.L., *et al*. (2012) A restricted subset of *var* genes mediates adherence of *Plasmodium falciparum*-infected erythrocytes to brain endothelial cells. *Proc Natl Acad Sci USA* **109:** 1782–1790.

Baptista, F.G., Pamplona, A., Pena, A.C., Mota, M.M., Pied, S., and Vigario, A.M. (2010) Accumulation of *Plasmodium berghei*-infected red blood cells in the brain is crucial for the development of cerebral malaria in mice. *Infect Immun* **78:** 4033–4039.

Bernabeu, M., Lopez, F.J., Ferrer, M., Martin-Jaular, L., Razaname, A., Corradin, G., *et al*. (2012) Functional analysis of *Plasmodium vivax* VIR proteins reveals different subcellular localizations and cytoadherence to the ICAM-1 endothelial receptor. *Cell Microbiol* **14:** 386–400.

Carvalho, B.O., Lopes, S.C., Nogueira, P.A., Orlandi, P.P., Bargieri, D.Y., Blanco, Y.C., *et al*. (2010) On the cytoadhesion of *Plasmodium vivax*-infected erythrocytes. *J Infect Dis* **202:** 638–647.

Claessens, A., Adams, Y., Ghumra, A., Lindergard, G., Buchan, C.C., Andisi, C., *et al*. (2012) A subset of group A-like *var* genes encodes the malaria parasite ligands for binding to human brain endothelial cells. *Proc Natl Acad Sci USA* **109:** 1772–1781.

Clark, I.A., Alleva, L.M., Budd, A.C., and Cowden, W.B. (2008) Understanding the role of inflammatory cytokines in malaria and related diseases. *Travel Med Infect Dis* **6:** 67–81.

Claser, C., Malleret, B., Gun, S.Y., Wong, A.Y., Chang, Z.W., Teo, P., *et al*. (2011) CD8+ T cells and IFN-gamma mediate the time-dependent accumulation of infected red blood cells in deep organs during experimental cerebral malaria. *PLoS ONE* **6:** e18720.

Combes, V., Rosenkranz, A.R., Redard, M., Pizzolato, G., Lepidi, H., Vestweber, D., *et al*. (2004) Pathogenic role of P-selectin in experimental cerebral malaria: importance of the endothelial compartment. *Am J Pathol* **164:** 781–786.

Cox, J., Semoff, S., and Hommel, M. (1987) *Plasmodium chabaudi*: a rodent malaria model for in-vivo and in-vitro cytoadherence of malaria parasites in the absence of knobs. *Parasite Immunol* **9:** 543–561.

Cox-Singh, J., Hiu, J., Lucas, S.B., Divis, P.C., Zulkarnaen, M., Chandran, P., *et al*. (2010) Severe malaria – a case of fatal *Plasmodium knowlesi* infection with post-mortem findings: a case report. *Malar J* **9:** 10.

Cunningham, D., Lawton, J., Jarra, W., Preiser, P., and Langhorne, J. (2010) The pir multigene family of *Plasmodium*: antigenic variation and beyond. *Mol Biochem Parasitol* **170:** 65–73.

De Brito, T., Barone, A.A., and Faria, R.M. (1969) Human liver biopsy in *P. falciparum* and *P. vivax* malaria. A light and electron microscopy study. *Virchows Arch A Pathol Pathol Anat* **348:** 220–229.

Desai, M., ter Kuile, F.O., Nosten, F., McGready, R., Asamoa, K., Brabin, B., and Newman, R.D. (2007) Epidemiology and burden of malaria in pregnancy. *Lancet Infect Dis* **7:** 93–104.

Field, J., and Shute, P. (1956) *Plasmodium vivax*.. In *The Microscopic Diagnosis of Human Malaria. Vol. 2: A Morphological Study of the Erythrocytic Parasites*. Studies from the Institute for Medical Research, Federation of Malaya. No. 24, p. 251. Kuala Lumpur.

Fonager, J., Pasini, E.M., Braks, J.A., Klop, O., Ramesar, J., Remarque, E.J., *et al*. (2012) Reduced CD36-dependent tissue sequestration of *Plasmodium*-infected erythrocytes is detrimental to malaria parasite growth *in vivo*. *J Exp Med* **209:** 93–107.

Franke-Fayard, B., Janse, C.J., Cunha-Rodrigues, M., Ramesar, J., Buscher, P., Que, I., *et al*. (2005) Murine malaria parasite sequestration: CD36 is the major receptor, but cerebral pathology is unlinked to sequestration. *Proc Natl Acad Sci USA* **102:** 11468–11473.

Freitas do Rosario, A.P., Lamb, T., Spence, P., Stephens, R., Lang, A., Roers, A., *et al*. (2012) IL-27 promotes IL-10 production by effector Th1 CD4+ T cells: a critical mechanism for protection from severe immunopathology during malaria infection. *J Immunol* **188:** 1178–1190.

Fu, Y., Ding, Y., Zhou, T.L., Ou, Q.Y., and Xu, W.Y. (2012) Comparative histopathology of mice infected with the 17XL and 17XNL strains of *Plasmodium yoelii*. *J Parasitol* **98:** 310–315.

Gilks, C.F., Walliker, D., and Newbold, C.I. (1990) Relationships between sequestration, antigenic variation and chronic parasitism in *Plasmodium chabaudi chabaudi* – a rodent malaria model. *Parasite Immunol* **12:** 45–64.

Haldar, K., Murphy, S.C., Milner, D.A., and Taylor, T.E. (2007) Malaria: mechanisms of erythrocytic infection and pathological correlates of severe disease. *Annu Rev Pathol* **2:** 217–249.

Huang, S., Hendriks, W., Althage, A., Hemmi, S., Bluethmann, H., Kamijo, R., *et al*. (1993) Immune response in mice that lack the interferon-gamma receptor. *Science* **259:** 1742–1745.

Kuhn, R., Lohler, J., Rennick, D., Rajewsky, K., and Muller, W. (1993) Interleukin-10-deficient mice develop chronic enterocolitis. *Cell* **75:** 263–274.

Lacerda, M.V., Fragoso, S.C., Alecrim, M.G., Alexandre, M.A., Magalhaes, B.M., Siqueira, A.M., *et al*. (2012) Post-mortem characterization of patients with clinical diagnosis of *Plasmodium vivax* malaria: to what extent does this parasite kill? *Clin Infect Dis* **55:** e67-74.

Langhorne, J., Ndungu, F.M., Sponaas, A.M., and Marsh, K. (2008) Immunity to malaria: more questions than answers. *Nat Immunol* **9:** 725–732.

Lawton, J., Brugat, T., Yan, Y.X., Reid, A.J., Bohme, U., Otto, T.D., *et al*. (2012) Characterization and gene expression

analysis of the cir multi-gene family of *Plasmodium chabaudi* chabaudi (AS). *BMC Genomics* **13:** 125.
Li, C., Sanni, L.A., Omer, F., Riley, E., and Langhorne, J. (2003) Pathology of *Plasmodium chabaudi* chabaudi infection and mortality in interleukin-10-deficient mice are ameliorated by anti-tumor necrosis factor alpha and exacerbated by anti-transforming growth factor beta antibodies. *Infect Immun* **71:** 4850–4856.
Lovegrove, F.E., Gharib, S.A., Pena-Castillo, L., Patel, S.N., Ruzinski, J.T., Hughes, T.R., *et al*. (2008) Parasite burden and CD36-mediated sequestration are determinants of acute lung injury in an experimental malaria model. *PLoS Pathog* **4:** e1000068.
Machado Siqueira, A., Lopes Magalhaes, B.M., Cardoso Melo, G., Ferrer, M., Castillo, P., Martin-Jaular, L., *et al*. (2012) Spleen rupture in a case of untreated *Plasmodium vivax* infection. *PLoS Negl Trop Dis* **6:** e1934.
Manning, L., Rosanas-Urgell, A., Laman, M., Edoni, H., McLean, C., Mueller, I., *et al*. (2012) A histopathologic study of fatal paediatric cerebral malaria caused by mixed *Plasmodium falciparum*/*Plasmodium vivax* infections. *Malar J* **11:** 107.
Martin-Jaular, L., Ferrer, M., Calvo, M., Rosanas-Urgell, A., Kalko, S., Graewe, S., *et al*. (2011) Strain-specific spleen remodelling in *Plasmodium yoelii* infections in Balb/c mice facilitates adherence and spleen macrophage-clearance escape. *Cell Microbiol* **13:** 109–122.
Mombaerts, P., Iacomini, J., Johnson, R.S., Herrup, K., Tonegawa, S., and Papaioannou, V. (1992) RAG-1-deficient mice have no mature B and T lymphocytes. *Cell* **68:** 869–877.
Mota, M.M., Jarra, W., Hirst, E., Patnaik, P.K., and Holder, A.A. (2000) *Plasmodium chabaudi*-infected erythrocytes adhere to CD36 and bind to microvascular endothelial cells in an organ-specific way. *Infect Immun* **68:** 4135–4144.
Nacer, A., Movila, A., Baer, K., Mikolajczak, S.A., Kappe, S.H., and Frevert, U. (2012) Neuroimmunological blood brain barrier opening in experimental cerebral malaria. *PLoS Pathog* **8:** e1002982.
Oh, P., Li, Y., Yu, J., Durr, E., Krasinska, K.M., Carver, L.A., *et al*. (2004) Subtractive proteomic mapping of the endothelial surface in lung and solid tumours for tissue-specific therapy. *Nature* **429:** 629–635.
Prudhomme, J.G., Sherman, I.W., Land, K.M., Moses, A.V., Stenglein, S., and Nelson, J.A. (1996) Studies of *Plasmodium falciparum* cytoadherence using immortalized human brain capillary endothelial cells. *Int J Parasitol* **26:** 647–655.
Rowe, J.A., Claessens, A., Corrigan, R.A., and Arman, M. (2009) Adhesion of *Plasmodium falciparum*-infected erythrocytes to human cells: molecular mechanisms and therapeutic implications. *Expert Rev Mol Med* **11:** e16.
Sanni, L.A., Jarra, W., Li, C., and Langhorne, J. (2004) Cerebral edema and cerebral hemorrhages in interleukin-10-deficient mice infected with *Plasmodium chabaudi*. *Infect Immun* **72:** 3054–3058.
Scudamore, C.L. (in press) Chapter 2 Practical approaches to reviewing and recording pathology data. In *A Practical Guide to the Histology of the Mouse*. Oxford: Wiley, pp. 33–39.
Shackelford, C., Long, G., Wolf, J., Okerberg, C., and Herbert, R. (2002) Qualitative and quantitative analysis of nonneoplastic lesions in toxicology studies. *Toxicol Pathol* **30:** 93–96.
Smith, L.P., Hunter, K.W., Oldfield, E.C., and Strickland, G.T. (1982) Murine malaria: blood clearance and organ sequestration of *Plasmodium yoelii*-infected erythrocytes. *Infect Immun* **38:** 162–167.
Spence, P.J., Cunningham, D., Jarra, W., Lawton, J., Langhorne, J., and Thompson, J. (2011) Transformation of the rodent malaria parasite *Plasmodium chabaudi*. *Nat Protoc* **6:** 553–561.
Stevenson, M.M., and Riley, E.M. (2004) Innate immunity to malaria. *Nat Rev Immunol* **4:** 169–180.
Taylor, T.E., Fu, W.J., Carr, R.A., Whitten, R.O., Mueller, J.S., Fosiko, N.G., *et al*. (2004) Differentiating the pathologies of cerebral malaria by postmortem parasite counts. *Nat Med* **10:** 143–145.
Weiss, L., Geduldig, U., and Weidanz, W. (1986) Mechanisms of splenic control of murine malaria: reticular cell activation and the development of a blood-spleen barrier. *Am J Anat* **176:** 251–285.
Whitten, R., Milner, D.A., Jr, Yeh, M.M., Kamiza, S., Molyneux, M.E., and Taylor, T.E. (2011) Liver pathology in Malawian children with fatal encephalopathy. *Hum Pathol* **42:** 1230–1239.

## Supporting information

Additional Supporting Information may be found in the online version of this article at the publisher's web-site:

**Fig. S1.** Parasite development, parasitemia and iRBC withdrawal in the peripheral blood. C57BL/6 mice were maintained in a reverse 12 h light–dark cycle and challenged with $10^5$ wild type *P. chabaudi* parasites. Tail blood was taken hourly between 9 h and 17 h, at days 8 and 11 post infection (p.i.). (A) Stages of differentiation and (B) parasitemia in the peripheral blood were measured. Each dot represents the average for at least six mice (± SEM). Statistical tests were made for each time point when compared with the parasitemia at 9.00 h. (C) Percentage of reduction of the peripheral parasitemia was analysed between 9.00 h and 12.00 h in each mouse. (D) Percentage of reduction of peripheral parasitemia was analysed in wild type mice or mice knocked out for IL10 ($il10^{-/-}$), IFNγ receptor ($ifn\gamma r^{-/-}$) or Rag1 ($rag1^{-/-}$, lacking T and B cells), all on C57BL/6 background. (*$P < 0.05$; **$P < 0.01$; ***$P < 0.001$, Mann–Whitney test).

**Fig. S2.** Imaging of *Plasmodium chabaudi* AS sequestration.
A. To assess the efficiency of our whole body perfusion, naïve C57BL/6 mice were perfused or not by intracardiac injection of PBS. Organ sections were then prepared and stained by H&E. Scale bars represent 100 μm.
B. C57BL/6 mice were also perfused 8 days post infection with $10^5$ wild type *Pcc*AS. Organs were then extracted and stained by H&E (i); scale bars represent 10 μm; arrows indicate infected red blood cells or (ii) and (iii) analysed by electron microscopy. Scale bars represent 1 μm (ii) and 0.5 μm (iii). Black arrows show close contact between infected red blood cells and the endothelial membrane.

**Fig. S3.** Development of imaging of bioluminescent parasites.
A. (i) To generate a vector that introduces the gene encoding

 

Luciferase into the *P.c. chabaudi* SSu-rRNA locus on chromosome 5, the pPc-$mCh_{CAM}$ plasmid vector (Spence *et al.*, 2011) was modified by excision of the BamH1-Not1 fragment of pPc-$mCh_{CAM}$ encoding mCherry and replacement with DNA encoding firefly luciferase. (ii) Southern blot analysis has been done to verify vector integration. Integration of pPc-$Luc_{CAM}$ into the *P. chabaudi ssu-rrna* locus on chromosome 5 results in an increase of KpnI restriction enzyme digestion product from 9.1kb to 19.7kb. K, Kpn1; S, SacII.

B. C57BL/6 and BALB/c mice were infected with $10^5$ *Pcc*AS*luc* parasites. The peripheral parasitemia, and luciferase activity (p/s) in the whole body, 8 days post infection, are presented here for 2 representative mice and indicate the discrepancy between these two values.

C. Luciferase activity (Relative Light Unit) according to the number of infected red blood cells (iRBCs) was assessed by Luciferase assay. The trendline is in red.

**Fig. S4.** Adaptive and inflammatory responses influence histopathological changes in the lungs during *Plasmodium chabaudi* AS infection. C57BL/6 mice wild type or knocked out for IL10 (*il10*$^{-/-}$), IFNγ receptor (*ifnγr*$^{-/-}$) or Rag1 (*rag1*$^{-/-}$, lacking T and B cells) were challenged with $10^5$ wild type *P. chabaudi* infected erythrocytes.

A. Increase of $CD4^+$ and $CD8^+$ T cells ($CD3^+$), macrophages (Mϕ; $CD11c^+$, $CD11b^{low/-}$, $F4/80^{int}$, $MHCII^+$), dendritic cells (DC; $CD11c^+$, $MHCII^{high}$), monocytes (Mo; $Ly6C^{high}$, $CD11b^+$, $Ly6G^-$) and neutrophils (Neu; $Ly6G^+$, $CD11b^+$, $Ly6C^{int}$) as analysed by flow cytometric analysis on the left lobe of the lungs of uninfected and *P. chabaudi* infected wild-type mice at days 5, 8 and 13.

B. Upper panel show a semi-quantitative measure of increased in alveolar septae cellularity described in *Experimental procedures*. Lower graphs show number of $CD4^+$ and $CD8^+$ T cells, macrophages, dendritic cells, monocytes and neutrophils, analysed by flow cytometric as described above.

C. Albumin in the BAL 9 days after a *P. chabaudi* infection. Each bar represents the average for at least six mice (± SEM). (*$P < 0.05$; **$P < 0.01$; ***$P < 0.001$, Mann–Whitney test).